Knockdown of ANLN inhibits the progression of lung adenocarcinoma via pyroptosis activation

LI SHENG[1*], YANHAI KANG[2*], DENGLIN CHEN[1] and LINYANG SHI[1]

Departments of [1]Medical Oncology and [2]Psychology, Hainan General Hospital, Hainan Affiliated Hospital of Hainan Medical University, Haikou, Hainan 570311, P.R. China

Received May 1, 2023; Accepted June 14, 2023

DOI: 10.3892/mmr.2023.13064

Abstract. Significant advancements have been achieved in the area of molecular targeted therapy for lung adenocarcinoma (LUAD). However, the complex molecular patterns and high heterogeneity of LUAD confine the efficacy of these therapies to a specific subset of patients; therefore, it is necessary to explore novel targets for LUAD treatment. The expression levels of anillin (ANLN) in LUAD were analyzed using the Gene Expression Profiling Interactive Analysis database. Furthermore, the association between ANLN gene expression and patient survival outcomes was evaluated using the Kaplan-Meier Plotter. Subsequently, small interfering RNA (siRNA) transfection was performed to knock down ANLN in A549 and H1299 cell lines, after which, TUNEL, colony formation and Transwell assays were conducted to assess cell death, colony formation and migration, respectively. Additionally, western blot analysis was performed to analyze the expression levels of caspase-1, interleukin (IL)-18 (IL-18), IL-1β, NLR family pyrin domain-containing 3 (NLRP3), apoptosis-associated speck-like protein containing a CARD domain (ASC) and cleaved gasdermin D (GSDMD) following ANLN knockdown. The results revealed that ANLN mRNA expression was significantly increased in LUAD tissues compared with adjacent normal samples. Furthermore, the expression levels of ANLN displayed an increasing trend with advancing clinical stage. Furthermore, patients with high ANLN expression levels exhibited poor overall survival rates compared with those with low ANLN expression levels. Subsequent ANLN knockdown experiments indicated elevated cell death rate, and reduced colony formation and migration in both A549 and H1299 cells. Additionally, ANLN knockdown resulted in increased protein expression levels of pyroptosis-associated molecules, including caspase-1, NLRP3, cleaved-GSDMD, IL-1β, ASC and IL-18 in both A549 and H1299 cells. In conclusion, ANLN represents an important gene and a promising therapeutic target for LUAD. Its potential as a therapeutic target makes it an interesting candidate for further exploration in the development of novel treatment strategies for LUAD.

Correspondence to: Professor Li Sheng, Department of Medical Oncology, Hainan General Hospital, Hainan Affiliated Hospital of Hainan Medical University, 19 Xiuhua Road, Xiuying, Haikou, Hainan 570311, P.R. China
E-mail: sl123_2007@163.com

*Contributed equally

Key words: lung adenocarcinoma, anillin, pyroptosis, tumor progression

Introduction

Lung cancer is a leading cause of cancer-associated mortality worldwide, and is frequently associated with a poor prognosis due to being diagnosed at an advanced stage (1). The most prevalent histological subtype of lung cancer is lung adenocarcinoma (LUAD), which accounts for ~60% of cases globally (2). In recent years, notable progress has been made in LUAD treatment with the use of molecular targeted therapies (3). Notably, small molecule-based targeted therapy has been shown to significantly improve the treatment outcomes of patients with carrying targetable molecular alterations, such as epidermal growth factor receptor (EGFR)-activating mutations, and anaplastic lymphoma kinase (ALK) and ROS1 translocations (4-6). Despite recent therapeutic advances, the worldwide 5-year survival rate for patients diagnosed with LUAD remains <20% (7). Consequently, chemotherapy remains the standard of care for these patients in routine clinical practice. To improve patient survival rates and quality of life, personalized molecular-targeted therapies are urgently required.

In order to identify potential therapeutic targets for LUAD, Gene Expression Profiling Interactive Analysis (GEPIA) was employed to investigate genes associated with LUAD prognosis. As a result, anillin (ANLN), an actin-binding protein with ubiquitous expression, was identified as a novel therapeutic target for LUAD (8). ANLN possesses multiple domains, including a myosin- and actin-binding domain, a RhoA-binding domain and a C-terminal pleckstrin homology domain (9,10). It has been demonstrated that ANLN serves a critical role in promoting tumor growth, migration and cytokinesis (11). Of particular note, ANLN has been suggested by several studies to be potentially involved in the pathogenesis of LUAD (12). Elevated levels of ANLN have been reported in LUAD cells, and it has been proposed that ANLN may serve

as a crucial determinant in distinguishing between low- and high-risk LUAD cases with unfavorable prognoses (12-15). Despite these findings, the precise biological functions and mechanisms underlying the involvement of ANLN in LUAD pathogenesis remain unknown, highlighting the need for further research in order to develop effective therapeutic strategies.

Pyroptosis is an inflammatory form of programmed cell death that features cell swelling, cell membrane rupture and the release of cytoplasmic contents, including pro-inflammatory molecules such as mature interleukin-1β and -18 (16). Studies have demonstrated that pyroptosis has a significant role in the pathogenesis of LUAD (17-20). Meanwhile, ANLN is known to have a role in regulating cellular behavior. However, the extent of ANLN's potential involvement in the pathogenesis of LUAD via the regulation of pyroptosis remains uncertain (21,22). Therefore, the present study aimed to explore the relationship between ANLN and pyroptosis in the progression of LUAD.

Materials and methods

Gene expression analysis using publicly available datasets. Gene expression levels of ANLN in tumors and adjacent normal samples were obtained from TCGA-LUAD dataset (accession no: 202208, 535 LUAD tissue samples and 59 adjacent normal samples). GEPIA (http://gepia.cancer-pku.cn/) was used for gene expression analysis. Kaplan-Meier analysis (http://kmplot.com/analysis/) was performed with TCGA-LUAD dataset (accession no: 202208). The log-rank test was used to assess the significance of between-group differences.

Cell lines and culture. The human LUAD cell lines A549 and H1299 were procured from The Cell Bank of Type Culture Collection of The Chinese Academy of Sciences, and were cultured in RPMI-1640 medium (cat. no. A1049101; Gibco; Thermo Fisher Scientific, Inc.) supplemented with 10% fetal bovine serum (FBS; cat. no. 10100147; Gibco; Thermo Fisher Scientific, Inc.) and penicillin (100 U/ml)/streptomycin (100 μg/ml) for <15 passages. The cells were authenticated by Shanghai Biowing Applied Biotechnology Co., Ltd. and were maintained under standard cell culture conditions at 37˚C in a humidified incubator with 5% CO_2.

Small interfering RNA (siRNA) transfection. In order to suppress ANLN expression, siRNA sequences were employed. Three distinct siRNA sequences were synthesized by Guangzhou Anernor Biotechnology Co., Ltd., as follows: si-ANLN #1 sense, 5'-GAGAGAAUCUUCAGAGAAAAA-3' and antisense, 5'-UUUUUCUCUGAAGAUUCUCUC-3'; si-ANLN #2 sense, 5'-GUGAAGAGAAAUCUUGUACAA-3' and antisense, 5'-UUGUACAAGAUUUCUCUUCAC-3'; si-ANLN #3 sense, 5'-CACUGAAGUAGAAGUUUCUAA-3' and antisense, 5'-UUAGAAACUUCUACUUCAGUG-3'; non-targeting negative control (NC) sense, 5'-UUCUCCGAACGAGUCACGU-3' and antisense, 5'-ACGUGACUCGUUCGGAGAA-3'. A549 and H1299 cells ($1x10^5$) were seeded in each well of a six-well plate. After 12 h, cells were transfected with 80 nM of control siRNA and ANLN siRNA. Lipofectamine® 2000 reagent (cat. no. 11668019; Invitrogen; Thermo Fisher Scientific, Inc.) was used for the transfection experiments (5 μl/well). After culture at 37˚C for 24 h, the transfection medium was replaced with fresh RPMI-1640 culture medium and the cells were further incubated at 37˚C for 48 h.

Western blot analysis. Proteins were extracted from A549 and H1299 cells using RIPA lysis buffer (Beyotime Institute of Biotechnology) containing 0.1 M PMSF and protease inhibitors (Roche Diagnostics). The protein concentration was determined using a BCA Protein Assay Kit (Shanghai Yeasen Biotechnology Co., Ltd.). Subsequently, the proteins (20 μg/lane) were separated by 10% SDS-PAGE, transferred onto PVDF membranes (MilliporeSigma) and blocked with 3% bovine serum albumin (cat. no. AR1006; Boster Biological Technology) for 2 h at room temperature. Primary antibodies against ANLN (cat. no. ab211872; Abcam; 1:1,000 dilution), GAPDH (cat. no. GB15002; Wuhan Servicebio Technology Co., Ltd.; 1:5,000 dilution), interleukin (IL)-18 (cat. no. ab243091; Abcam; 1:1,000 dilution), apoptosis-associated speck-like protein containing a CARD domain (ASC; cat. no. ab283684; Abcam; 1:1,000 dilution), pro-caspase-1 (cat. no. ab179515; Abcam; 1:1,000 dilution), caspase-1 (cat. no. ab207802; Abcam; 1:1,000 dilution), NLR pyrin domain-containing (NLRP)3 (cat. no. ab263899; Abcam; 1:1,000 dilution), cleaved-gasdermin D (GSDMD; cat. no. ab215203; Abcam; 1:1,000 dilution) and IL-1β (cat. no. ab254360; Abcam; 1:1,000 dilution) were incubated with the membranes overnight at 4˚C. After washing with TBST (1X) containing 0.3% Tween-20, the membranes were incubated with horseradish peroxidase-conjugated secondary antibodies (cat. no. 074-1506 and 074-1807; KPL; 1:5,000 dilution) for 2 h at room temperature. Immunoreactive bands were visualized using an ECL kit (Beyotime Institute of Biotechnology) and were semi-quantified using Image J software (Image J 1.8.0; National Institutes of Health).

RNA isolation and reverse transcription-quantitative PCR (RT-qPCR). Total RNA was extracted from A549 and H1299 cells using TRIzol® reagent (Invitrogen; Thermo Fisher Scientific, Inc.) and reverse transcribed into cDNA with the PrimeScript™ RT reagent Kit (Takara Biotechnology Co., Ltd.), according to the manufacturer's instructions. qPCR was performed on an ABI 7900HT PCR system (Applied Biosystems; Thermo Fisher Scientific, Inc.) using TB Green® Premix Ex Taq™ II (Takara Biotechnology Co., Ltd.). The primer sequences for qPCR were as follows: ANLN forward, 5'-CGCCTCAGACTCCTGGTTTT-3' and reverse, 5'-GCTCCAGCAGTTTCTCCGTA-3'; GAPDH forward, 5'-AATGGGCAGCCGTTAGGAAA-3' and reverse, 5'-GCGCCCAATACGACCAAATC-3'. Amplifications were performed following the procedure of a two-step method (95˚C for 30 sec, 1 cycle; followed by 40 cycles of 95˚C for 10 sec and 60˚C for 30 sec; and melting curve stage). The fold change in mRNA expression levels was calculated using the $2^{-\Delta\Delta Cq}$ method and normalized to GAPDH (23).

Colony formation assay. A549 and H1299 cells with ANLN knockdown were seeded at a density of 500 cells/well in 12-well plates and were incubated for 14 days at 37˚C with

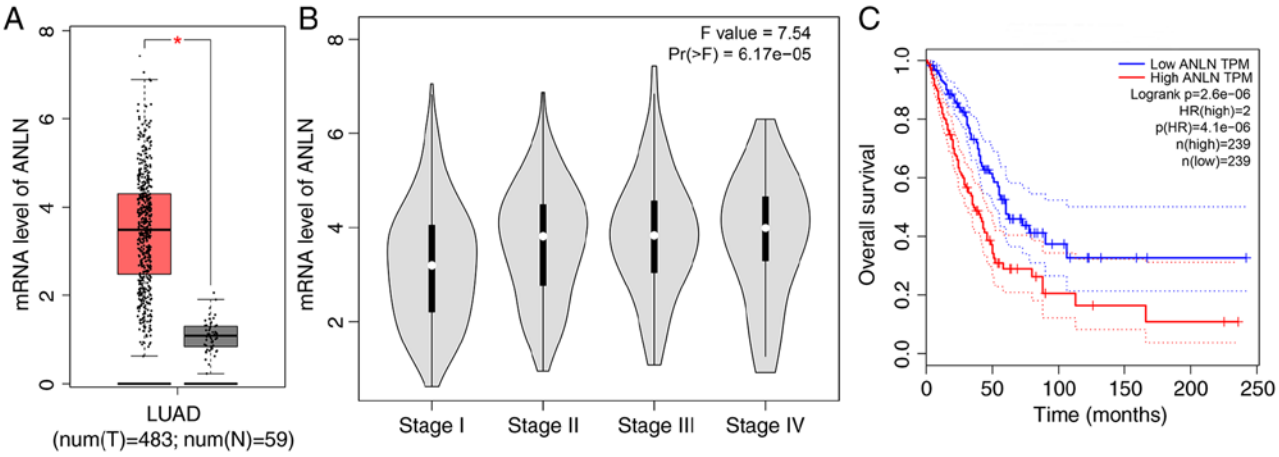

Figure 1. ANLN is upregulated and serves as a prognostic factor in LUAD. (A) ANLN mRNA expression in LUAD tissues and normal tissues in The Cancer Genome Atlas database. *P<0.05. (B) ANLN mRNA expression increased with TNM stage ($P=6.17x10^{-5}$). (C) Kaplan-Meier analysis of the overall survival of patients with LUAD based on ANLN expression ($P=4.1x10^{-6}$). ANLN, anillin; LUAD, lung adenocarcinoma; HR, hazard ratio.

5% CO_2 in a humidified incubator. Subsequently, the culture medium was discarded and the cells were washed with PBS. Following fixation with 4% paraformaldehyde at room temperature for 30 min, the cells were stained using Giemsa stain solution at room temperature for 60 min. Finally, the colonies were manually counted. A cluster with >50 cells was considered a colony.

TUNEL staining. Cell death was evaluated using TUNEL staining, which was performed with an *In Situ* Cell Death Detection kit (Roche Diagnostics) according to the manufacturer's protocol. A549 and H1299 cells ($1x10^5$) were seeded in each well of a six-well plate and cultured at 37˚C for 48 h. Then the cells were fixed on coverslips with 4% paraformaldehyde at room temperature for 30 min and subsequently treated with 0.1% Triton X-100 for 10 min at room temperature. The cells were then washed with PBS and incubated with 50 μl TUNEL reaction mixture at 37˚C for 1 h, followed by counterstaining with DAPI (1:100) for 10 min at room temperature. Finally, the cells were mounted with ProLong Gold antifade reagent (Invitrogen; Thermo Fisher Scientific, Inc.). Visualization of the cells was achieved using an inverted fluorescence microscope (Nikon Corporation) and three random fields of view were observed.

Transwell assay. The migration of A549 and H1299 cells was assessed using a Transwell kit (cat. no. 354480, Corning, Inc.). Specifically, $5x10^4$ cells were suspended in 300 μl serum-free medium and seeded into the upper chamber of the Transwell with 8-μm pore chambers inserted into 24-well plates, whereas 500 μl medium containing 30% FBS was added to the lower chamber. Following a 48-h incubation period at 37˚C, the migrated cells on the underside of the membrane were fixed with 0.5% crystal violet at room temperature for 30 min, washed with PBS and air-dried. Images of six randomly selected fields were captured under a light microscope and the number of migrated cells was determined.

Statistical analysis. Statistical analysis was conducted using GraphPad Prism software (version 9.0; GraphPad Software, Inc.). All experiments were repeated three times and data are expressed as the mean ± standard deviation. Two-group comparisons were analyzed using the unpaired Student's t-test, whereas one-way ANOVA followed by Tukey's post-hoc test was use for multiple comparisons. P<0.05 was considered to indicate a statistically significant difference.

Results

High expression of ANLN is associated with a poor prognosis in LUAD. Using The Cancer Genome Atlas (TCGA) database (https://www.cancer.gov/ccg/research/genome-sequencing/tcga), a significant increase in the mRNA expression levels of ANLN was detected in LUAD tissues compared with adjacent normal samples (P<0.05; Fig. 1A). Subsequently, by analyzing TCGA and Genotype-Tissue Expression databases on the GEPIA website, it was revealed that the mRNA expression levels of ANLN were high in LUAD and were gradually increased with advancing clinical stage (Fig. 1B). Moreover, Kaplan-Meier Plotter database analysis revealed that patients with high ANLN expression had significantly poorer overall survival (OS) than those expressing low levels of ANLN (HR=2, log-rank $P=2.6x10^{-6}$; Fig. 1C). Collectively, these findings suggested that ANLN may serve as a promoter gene in LUAD.

Knockdown of ANLN promotes cell death, and suppresses the colony formation and migration of A549 and H1299 cells. To investigate the potential role of ANLN in LUAD, the present study transfected A549 and H1299 cells with an ANLN siRNA. As demonstrated by qPCR and western blot analysis, the mRNA and protein expression levels of ANLN were significantly decreased in the ANLN knockdown groups compared with those in the NC groups (Fig. 2A and B), indicating that ANLN was effectively downregulated in these cells. Moreover, TUNEL/DAPI double staining revealed a marked increase in the number of TUNEL-positive dead cells in the ANLN knockdown groups compared with in the NC groups (Fig. 3A). In addition, the colony-forming ability of A549 and H1299 cells was significantly reduced

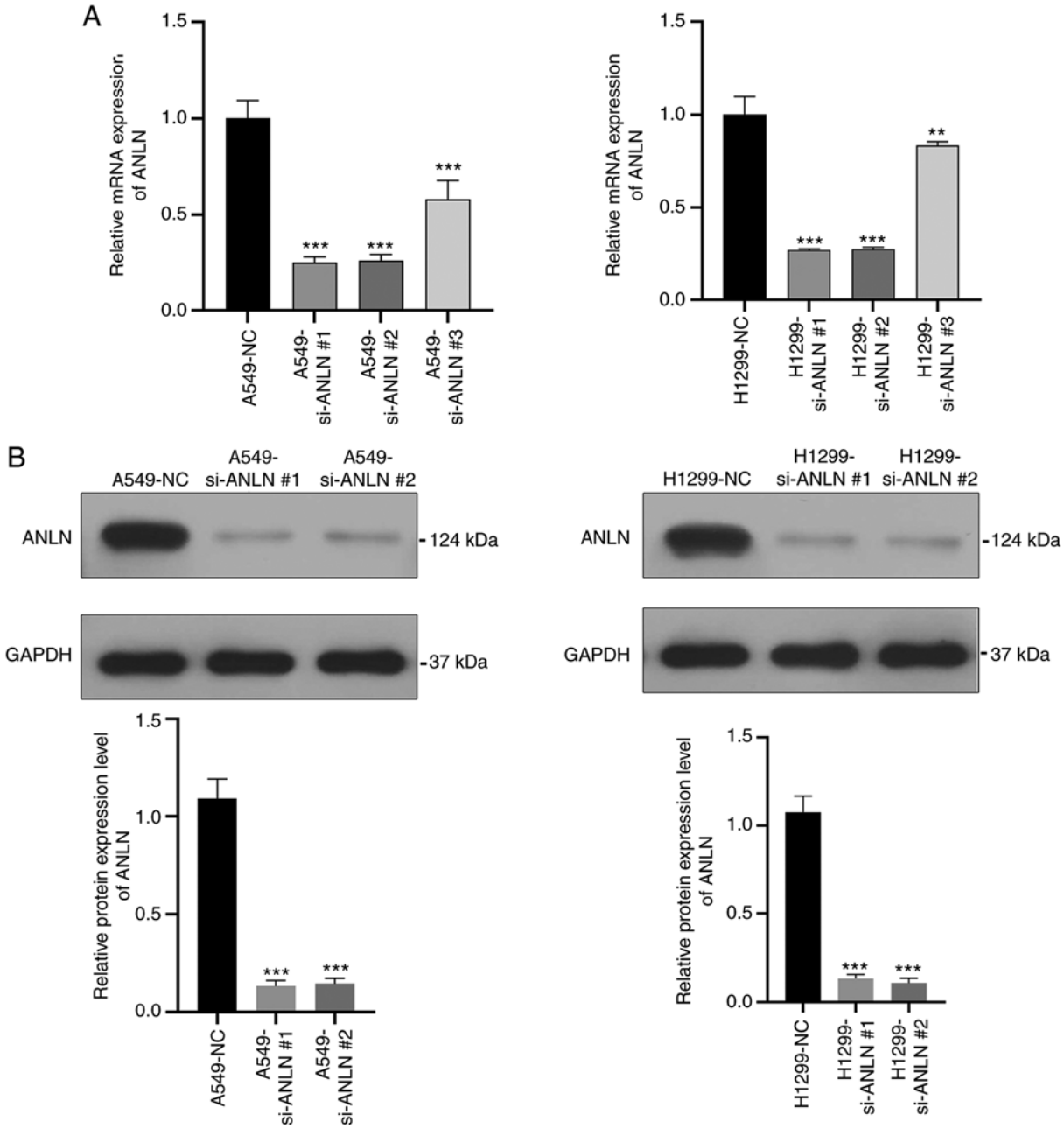

Figure 2. Successful knockdown of ANLN in A549 and H1299 cells. (A) Reverse transcription-quantitative PCR confirming successful siRNA-induced knockdown of ANLN in A549 and H1299 cells. (B) Protein expression levels of ANLN in A549 and H1299 cells were determined by western blotting. Grayscale analysis was performed using ImageJ software. Data are presented as the mean ± SD (n=3). **P<0.01, ***P<0.001 vs. NC. ANLN, anillin; NC, negative control; si, small interfering.

upon ANLN silencing compared with that in the NC groups (Fig. 3B). Furthermore, knockdown of ANLN in A549 and H1299 cells significantly attenuated cell migration compared with that in the NC groups, as confirmed by Transwell assays (Fig. 3C).

Knockdown of ANLN potentiates pyroptosis in A549 and H1299 cells. The present study analyzed the expression of pyroptosis-associated proteins to investigate the potential effects of ANLN on cell viability through a pyroptosis-dependent mechanism. The results indicated that ANLN knockdown led to an increase in the expression levels of inflammasome/pyroptosis-related proteins, such as caspase-1, NLRP3, cleaved-GSDMD, IL-1β, ASC and IL-18, thus suggesting that the knockdown of ANLN may trigger pyroptosis in A549 and H1299 cells (Fig. 4A and B).

Discussion

The aim of the present study was to identify a potential therapeutic target for patients with LUAD, a type of lung cancer that accounts for ~60% of all cases and has a 5-year survival rate of <20% (2,7). Although significant progress has been made in the molecular targeted therapy of LUAD, particularly for those with specific mutations in EGFR, ALK, RET and ROS1 (3,24-27), the high heterogeneity and complex molecular

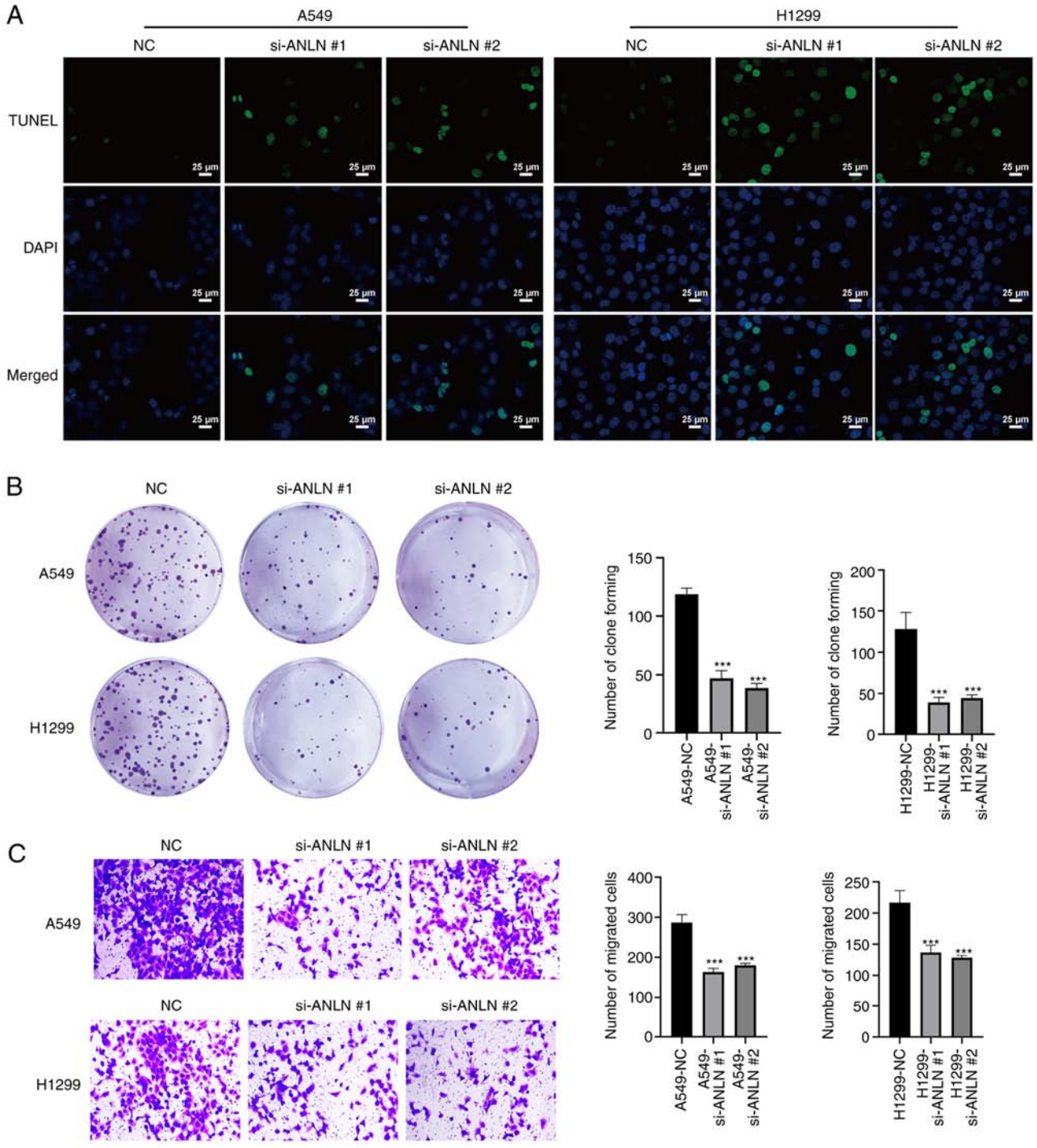

Figure 3. ANLN promotes cell death, and suppresses the colony formation and migration of A549 and H1299 cells. (A) A549 and H1299 cell death was detected by TUNEL assay (scale bars, 25 μm). (B) Colony-forming ability of A549 and H1299 cells was detected by colony formation assay. (C) Migration of A549 and H1299 cells was evaluated by Transwell assay (magnification, x100). Data are presented as the mean ± SD (n=3). ***P<0.001 vs. NC. ANLN, anillin; NC, negative control; si, small interfering.

patterns of LUAD limit the applicability of these targeted therapies, thus leaving a number of patients without effective treatment options (28). Therefore, it is critical to discover new targets for the treatment of LUAD.

ANLN, an actin-binding protein involved in cell division, serves a crucial role in cell proliferation and migration (29). Notably, localization of ANLN varies during different phases of the cell cycle. During interphase, the ANLN protein is localized exclusively in the nucleus, whereas it becomes cytoplasmic during mitosis (30). Furthermore, ANLN has been identified as a poor prognostic marker associated with aggressive cancer phenotypes in multiple types of cancer, including bladder cancer (31), hepatocellular carcinoma (32), colorectal cancer (33), head and neck squamous cell carcinoma (34) and stage I LUAD (14). The present study demonstrated that high ANLN expression was significantly associated with clinical stage progression in patients with LUAD and that those exhibiting higher expression levels of

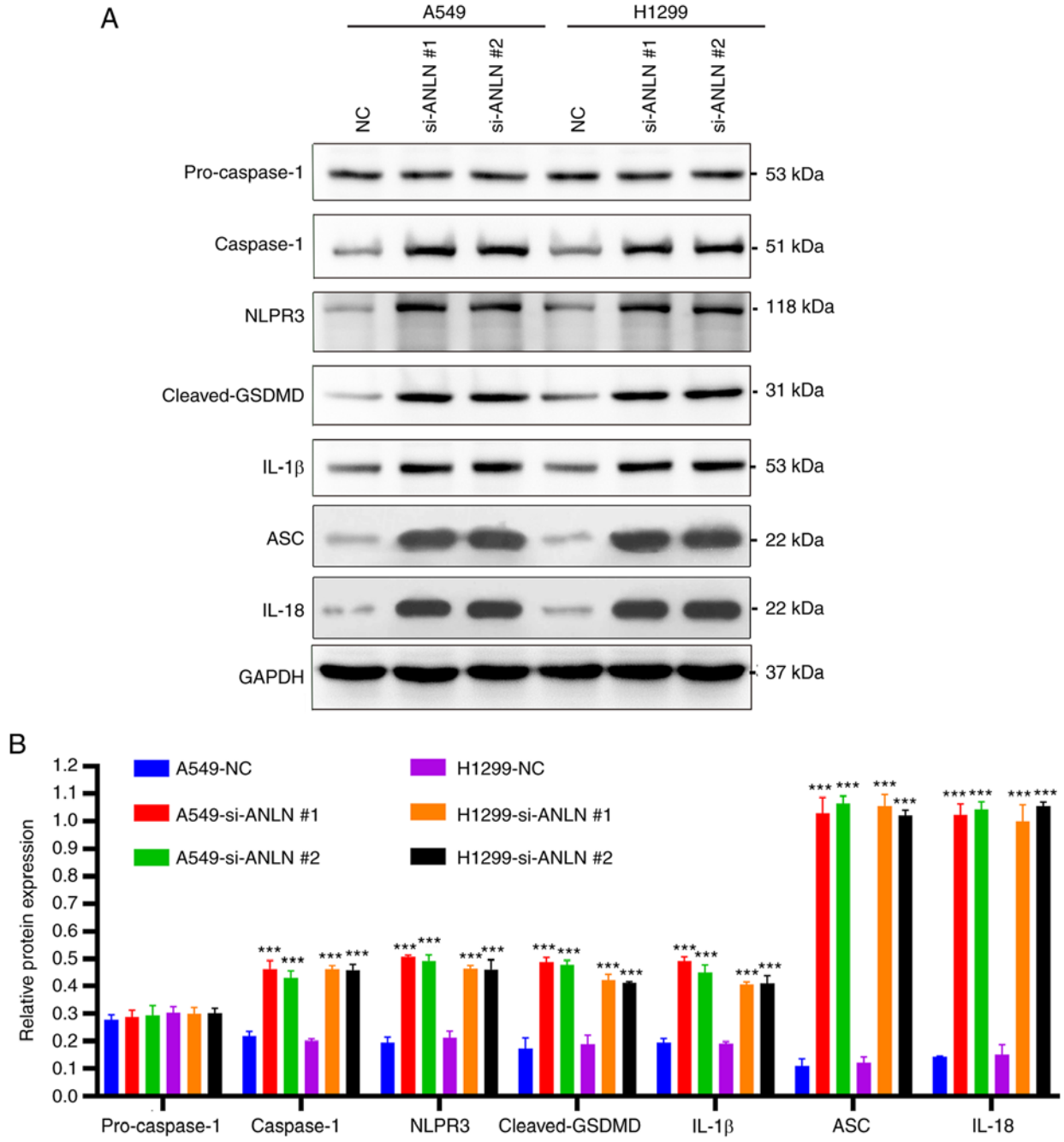

Figure 4. ANLN knockdown induces pyroptosis in A549 and H1299 cells. (A) Protein expression levels of pro-caspase-1, caspase-1, NLRP3, cleaved-GSDMD, IL-1β, ASC and IL-18 protein level in A549 and H1299 cells were detected by western blot analysis. (B) Grayscale analysis was performed by ImageJ software. Data are presented as the mean ± SD (n=3). ***P<0.001 vs. NC. ANLN, anillin; ASC, apoptosis-associated speck-like protein containing a CARD domain; GSDMD, gasdermin D; IL, interleukin; NC, negative control; NRP3, NLR family pyrin domain-containing 3; si, small interfering.

ANLN had poorer prognoses. These findings are consistent with previously reported results, which suggest that ANLN could serve as a novel prognostic indicator for patients with LUAD.

As an actin-binding protein, ANLN has a crucial role in regulating various cellular processes, such as cell proliferation, apoptosis and invasion. Silencing ANLN in colorectal carcinoma cell lines has been reported to result in reduced proliferation *in vitro* and *in vivo*, along with induction of G_0/G_1 cell cycle arrest (35). Similarly, knockdown of ANLN in breast cancer cells was shown to markedly inhibit cell proliferation, migration and invasion, leading to cell cycle arrest in the G_2/M phase and the induction of apoptosis (36). Exosomal ANLN-210 has also been found to promote macrophage polarization via the PTEN/PI3K/Akt signaling pathway, thereby stimulating tumor growth in head and neck squamous cell carcinoma (34). The present study confirmed that silencing ANLN markedly increased cell death, and suppressed the colony formation and migration of A549 and H1299 cells, highlighting the potential therapeutic significance of targeting ANLN in LUAD.

Pyroptosis is a unique form of programmed cell death that is highly dependent on inflammation, which is distinct from apoptosis (37). Pyroptosis can be induced

via caspase-1 (mammals), human caspase-4 and caspase-5, or mouse caspase-11 (38). Inflammasomes, such as the NLRP3 inflammasome, initiate caspase-1 activation (39,40), and the adaptor protein ASC facilitates the interaction between NLRP3 and caspase-1 (41,42). Upon activation, caspase-1 cleaves GSDMD to generate the N-terminal fragment of GSDMD (GSDMD-N), which is crucial for pyroptosis (43). GSDMD-N interacts with the lipids of the inner membrane, leading to pore formation in the plasma membrane, ultimately causing cellular swelling and rupture, and the release of pro-inflammatory cytokines, resulting in pyroptotic cell death (44,45). Previous studies have reported the induction of pyroptosis in endothelial and bronchial epithelial cells through caspase-1 activation. For example, caspase-1 inflammasome activation has been shown to mediate homocysteine-induced pyroptosis in endothelial cells (46). Similarly, cigarette smoke extract can induce pyroptosis in human bronchial epithelial cells via the ROS/NLRP3/caspase-1 pathway (47). WSPM2.5 also induces pyroptosis through caspase-1/IL-1β/IL-18- and ATP/P2Y-dependent mechanisms in human bronchial epithelial cells (48). The present study revealed that ANLN knockdown increased the protein expression levels of caspase-1, which suggests that caspase-1 activation may be involved in ANLN knockdown-induced pyroptosis in A549 and H1299 cells. Human caspase-4 and caspase-5, or mouse caspase-11, can directly cleave GSDMD to induce pyroptosis (38). In the context of Caspase-1-independent pyroptosis, caspase-4, caspase-5 and caspase-11 serve as initiating activators and directly recognize LPS from gram-negative bacteria in the host cytoplasm through their CARD domains (49). Although caspase-4 has been suggested to cleave pro-IL-1β and pro-IL-18 in epithelial cells, further confirmation of this finding is required (50).

Analysis of prognosis has revealed a lower survival rate in patients with LUAD who exhibit low expression levels of NLRP7, NLRP1, NLRP2 and nucleotide binding oligomerization domain containing 1, as well as high expression levels of caspase-6 (17). Additionally, activation of the NLRP3 inflammasome has been shown to accelerate the progression of LUAD by promoting the proliferation and metastasis of lung cancer cells (18). Conversely, downregulation of GSDMD has been demonstrated to mitigate tumor proliferation via the intrinsic mitochondrial apoptotic pathway, as well as through inhibition of EGFR/Akt signaling, and is associated with favorable prognostic outcomes in LUAD (19,20). In the current study, it was revealed that knockdown of ANLN significantly increased the expression levels of caspase-1, NLRP3, cleaved-GSDMD, IL-1β, ASC and IL-18 in A549 and H1299 cells. These findings suggested that silencing ANLN may have a critical role in promoting pyroptotic cell death in LUAD. Therefore, these data demonstrated that ANLN knockdown could lead to pyroptosis in A549 and H1299 cells, which may affect the progression of LUAD.

In conclusion, knockdown of ANLN can significantly disrupt the progression of LUAD by inducing pyroptosis, and suppressing the colony formation and migration of A549 and H1299 cells. These findings indicated that ANLN may serve as a promising therapeutic target for the treatment of LUAD.

Acknowledgements

Not applicable.

Funding

This work was supported by the Key Research and Development Program of Hainan Province, China (grant no. ZDYF2019189).

Availability of data and materials

The datasets used and/or analyzed during the present study are available from the corresponding author on reasonable request.

Authors' contributions

LS, YK and DC conceived and designed this study. LS, YK and LYS carried out the analyses and also participated in the study design. LS wrote the manuscript. YK and LS confirm the authenticity of all the raw data. All authors read and approved the final manuscript.

Ethics approval and consent to participate

Not applicable.

Patient consent for publication

Not applicable.

Competing interests

The authors declare that they have no competing interests.

References

1. Szczepanski AP, Tsuboyama N, Watanabe J, Hashizume R, Zhao Z and Wang L: POU2AF2/C11orf53 functions as a coactivator of POU2F3 by maintaining chromatin accessibility and enhancer activity. Sci Adv 8: eabq2403, 2022.
2. Wang Y, Ren F, Sun D, Liu J, Liu B, He Y, Pang S, Shi B, Zhou F, Yao L, *et al*: CircKEAP1 suppresses the progression of lung adenocarcinoma via the miR-141-3p/KEAP1/NRF2 axis. Front Oncol 11: 672586, 2021.
3. Yuan J, Yuan B, Zeng L, Liu B, Chen Y, Meng X, Sun R, Lv X, Wang W and Yang S: Identification and validation of tumor microenvironment-related genes of prognostic value in lung adenocarcinoma. Oncol Lett 20: 1772-1780, 2020.
4. Soria JC, Ohe Y, Vansteenkiste J, Reungwetwattana T, Chewaskulyong B, Lee KH, Dechaphunkul A, Imamura F, Nogami N, Kurata T, *et al*: Osimertinib in untreated EGFR-mutated advanced non-small-cell lung cancer. N Engl J Med 378: 113-125, 2018.
5. Solomon BJ, Mok T, Kim DW, Wu YL, Nakagawa K, Mekhail T, Felip E, Cappuzzo F, Paolini J, Usari T, *et al*: First-line crizotinib versus chemotherapy in ALK-positive lung cancer. N Engl J Med 371: 2167-2177, 2014.
6. Mazières J, Zalcman G, Crinò L, Biondani P, Barlesi F, Filleron T, Dingemans AM, Léna H, Monnet I, Rothschild SI, *et al*: Crizotinib therapy for advanced lung adenocarcinoma and a ROS1 rearrangement: Results from the EUROS1 cohort. J Clin Oncol 33: 992-999, 2015.
7. Miller KD, Nogueira L, Devasia T, Mariotto AB, Yabroff KR, Jemal A, Kramer J and Siegel RL: Cancer treatment and survivorship statistics, 2022. CA Cancer J Clin 72: 409-436, 2022.

8. Jia H, Gao Z, Yu F, Guo H and Li B: Actin-binding protein anillin promotes the progression of hepatocellular carcinoma *in vitro* and in mice. Exp Ther Med 21: 454, 2021.
9. Strausberg RL, Feingold EA, Grouse LH, Derge JG, Klausner RD, Collins FS, Wagner L, Shenmen CM, Schuler GD, Altschul SF, *et al*: Generation and initial analysis of more than 15,000 full-length human and mouse cDNA sequences. Proc Natl Acad Sci USA 99: 16899-16903, 2002.
10. Ota T, Suzuki Y, Nishikawa T, Otsuki T, Sugiyama T, Irie R, Wakamatsu A, Hayashi K, Sato H, Nagai K, *et al*: Complete sequencing and characterization of 21,243 full-length human cDNAs. Nat Genet 36: 40-45, 2004.
11. Lian YF, Huang YL, Wang JL, Deng MH, Xia TL, Zeng MS, Chen MS, Wang HB and Huang YH: Anillin is required for tumor growth and regulated by miR-15a/miR-16-1 in HBV-related hepatocellular carcinoma. Aging (Albany NY) 10: 1884-1901, 2018.
12. Deng F, Xu Z, Zhou J, Zhang R and Gong X: ANLN Regulated by miR-30a-5p mediates malignant progression of lung adenocarcinoma. Comput Math Methods Med 2021: 9549287, 2021.
13. Luo C, Lei M, Zhang Y, Zhang Q, Li L, Lian J, Liu S, Wang L, Pi G and Zhang Y: Systematic construction and validation of an immune prognostic model for lung adenocarcinoma. J Cell Mol Med 24: 1233-1244, 2020.
14. Deng Y, Chen X, Huang C, Song J, Feng S, Chen X and Zhou R: Screening and validation of significant genes with poor prognosis in pathologic stage-I lung adenocarcinoma. J Oncol 2022: 3794021, 2022.
15. Zhang L, Luo Y, Cheng T, Chen J, Yang H, Wen X, Jiang Z, Li H and Pan C: Development and validation of a prognostic N6-methyladenosine-related immune gene signature for lung adenocarcinoma. Pharmgenomics Pers Med 14: 1549-1563, 2021.
16. Broz P, Pelegrin P and Shao F: The gasdermins, a protein family executing cell death and inflammation. Nat Rev Immunol 20: 143-157, 2020.
17. Lin W, Chen Y, Wu B, Chen Y and Li Z: Identification of the pyroptosis-related prognostic gene signature and the associated regulation axis in lung adenocarcinoma. Cell Death Discov 7: 161, 2021.
18. Gu H, Deng W, Zhang Y, Chang Y, Shelat VG, Tsuchida K, Lino-Silva LS and Wang Z: NLRP3 activation in tumor-associated macrophages enhances lung metastasis of pancreatic ductal adenocarcinoma. Transl Lung Cancer Res 11: 858-868, 2022.
19. Gao J, Qiu X, Xi G, Liu H, Zhang F, Lv T and Song Y: Downregulation of GSDMD attenuates tumor proliferation via the intrinsic mitochondrial apoptotic pathway and inhibition of EGFR/Akt signaling and predicts a good prognosis in non-small cell lung cancer. Oncol Rep 40: 1971-1984, 2018.
20. Wang Y, Kong H, Zeng X, Liu W, Wang Z, Yan X, Wang H and Xie W: Activation of NLRP3 inflammasome enhances the proliferation and migration of A549 lung cancer cells. Oncol Rep 35: 2053-2064, 2016.
21. Dai X, Chen X, Hakizimana O and Mei Y: Genetic interactions between ANLN and KDR are prognostic for breast cancer survival. Oncol Rep 42: 2255-2266, 2019.
22. Wang Y, Zhang JW, Wang JW, Wang JL, Zhang SC, Ma RY, Zhang J, Li Y, Liu PJ, Xue WJ, *et al*: BMSCs overexpressed ISL1 reduces the apoptosis of islet cells through ANLN carrying exosome, INHBA, and caffeine. Cell Mol Life Sci 79: 538, 2022.
23. Livak KJ and Schmittgen TD: Analysis of relative gene expression data using real-time quantitative PCR and the 2(-Delta Delta C(T)) method. Methods 25: 402-408, 2001.
24. Harrison PT, Vyse S and Huang PH: Rare epidermal growth factor receptor (EGFR) mutations in non-small cell lung cancer. Semin Cancer Biol 61: 167-179, 2020.
25. Muller IB, de Langen AJ, Giovannetti E and Peters GJ: Anaplastic lymphoma kinase inhibition in metastatic non-small cell lung cancer: Clinical impact of alectinib. Onco Targets Ther 10: 4535-4541, 2017.
26. Drilon A, Wang L, Hasanovic A, Suehara Y, Lipson D, Stephens P, Ross J, Miller V, Ginsberg M, Zakowski MF, *et al*: Response to Cabozantinib in patients with RET fusion-positive lung adenocarcinomas. Cancer Discov 3: 630-635, 2013.
27. Bergethon K, Shaw AT, Ou SH, Katayama R, Lovly CM, McDonald NT, Massion PP, Siwak-Tapp C, Gonzalez A, Fang R, *et al*: ROS1 rearrangements define a unique molecular class of lung cancers. J Clin Oncol 30: 863-870, 2012.
28. Tan AC and Tan DSW: Targeted therapies for lung cancer patients with oncogenic driver molecular alterations. J Clin Oncol 40: 611-625, 2022.
29. Hall G, Lane BM, Khan K, Pediaditakis I, Xiao J, Wu G, Wang L, Kovalik ME, Chryst-Stangl M, Davis EE, *et al*: The human FSGS-causing ANLN R431C mutation induces dysregulated PI3K/AKT/mTOR/Rac1 signaling in podocytes. J Am Soc Nephrol 29: 2110-2122, 2018.
30. Shi Y, Ma X, Wang M, Lan S, Jian H, Wang Y, Wei Q and Zhong F: Comprehensive analyses reveal the carcinogenic and immunological roles of ANLN in human cancers. Cancer Cell Int 22: 188, 2022.
31. Wang Y, Chen L, Ju L, Qian K, Liu X, Wang X and Xiao Y: Novel biomarkers associated with progression and prognosis of bladder cancer identified by co-expression analysis. Front Oncol 9: 1030, 2019.
32. Zhang F, Cai J, Hu K, Liu W, Lu S, Tang B, Li M, Wu W, Ren Z and Yin X: An immune-related gene signature predicting prognosis and immunotherapy response in hepatocellular carcinoma. Comb Chem High Throughput Screen 25: 2203-2216, 2022.
33. Wang G, Shen W, Cui L, Chen W, Hu X and Fu J: Overexpression of Anillin (ANLN) is correlated with colorectal cancer progression and poor prognosis. Cancer Biomark 16: 459-465, 2016.
34. Guo E, Mao X, Wang X, Guo L, An C, Zhang C, Song K, Wang G, Duan C, Zhang X, *et al*: Alternatively spliced ANLN isoforms synergistically contribute to the progression of head and neck squamous cell carcinoma. Cell Death Dis 12: 764, 2021.
35. Liu Y, Cao P, Cao F, Wang S, He Y, Xu Y and Wang Y: ANLN, regulated by SP2, promotes colorectal carcinoma cell proliferation via PI3K/AKT and MAPK signaling pathway. J Invest Surg 35: 268-277, 2022.
36. Wang Z, Hu S, Li X, Liu Z, Han D, Wang Y, Wei L, Zhang G and Wang X: MiR-16-5p suppresses breast cancer proliferation by targeting ANLN. BMC Cancer 21: 1188, 2021.
37. Yu P, Zhang X, Liu N, Tang L, Peng C and Chen X: Pyroptosis: Mechanisms and diseases. Signal Transduct Target Ther 6: 128, 2021.
38. Man SM and Kanneganti TD: Converging roles of caspases in inflammasome activation, cell death and innate immunity. Nat Rev Immunol 16: 7-21, 2016.
39. Brocker CN, Kim D, Melia T, Karri K, Velenosi TJ, Takahashi S, Aibara D, Bonzo JA, Levi M, Waxman DJ and Gonzalez FJ: Long non-coding RNA Gm15441 attenuates hepatic inflammasome activation in response to PPARA agonism and fasting. Nat Commun 11: 5847, 2020.
40. Tsuchiya K, Nakajima S, Hosojima S, Thi Nguyen D, Hattori T, Manh Le T, Hori O, Mahib MR, Yamaguchi Y, Miura M, *et al*: Caspase-1 initiates apoptosis in the absence of gasdermin D. Nat Commun 10: 2091, 2019.
41. Paik S, Kim JK, Silwal P, Sasakawa C and Jo EK: An update on the regulatory mechanisms of NLRP3 inflammasome activation. Cell Mol Immunol 18: 1141-1160, 2021.
42. Looi CK, Hii LW, Chung FF, Mai CW, Lim WM and Leong CO: Roles of inflammasomes in Epstein-Barr virus-associated nasopharyngeal cancer. Cancers (Basel) 13: 1786, 2021.
43. Shi J, Zhao Y, Wang K, Shi X, Wang Y, Huang H, Zhuang Y, Cai T, Wang F and Shao F: Cleavage of GSDMD by inflammatory caspases determines pyroptotic cell death. Nature 526: 660-665, 2015.
44. Evavold CL, Hafner-Bratkovič I, Devant P, D'Andrea JM, Ngwa EM, Boršić E, Doench JG, LaFleur MW, Sharpe AH, Thiagarajah JR and Kagan JC: Control of gasdermin D oligomerization and pyroptosis by the Ragulator-Rag-mTORC1 pathway. Cell 184: 4495-4511.e19, 2021.
45. de Vasconcelos NM, Van Opdenbosch N, Van Gorp H, Parthoens E and Lamkanfi M: Single-cell analysis of pyroptosis dynamics reveals conserved GSDMD-mediated subcellular events that precede plasma membrane rupture. Cell Death Differ 26: 146-161, 2019.
46. Xi H, Zhang Y, Xu Y, Yang WY, Jiang X, Sha X, Cheng X, Wang J, Qin X, Yu J, *et al*: Caspase-1 inflammasome activation mediates homocysteine-induced pyrop-apoptosis in endothelial cells. Circ Res 118: 1525-1539, 2016.

47. Zhang MY, Jiang YX, Yang YC, Liu JY, Huo C, Ji XL and Qu YQ: Cigarette smoke extract induces pyroptosis in human bronchial epithelial cells through the ROS/NLRP3/caspase-1 pathway. Life Sci 269: 119090, 2021.
48. Fu X, Hong W, Li S, Chen Z, Zhou W, Dai J, Deng X, Zhou H, Li B and Ran P: Wood smoke particulate matter (WSPM2.5) induces pyroptosis through both caspase-1/IL-1β/IL-18 and ATP/P2Y-dependent mechanisms in human bronchial epithelial cells. Chemosphere 307: 135726, 2022.
49. Kayagaki N, Wong MT, Stowe IB, Ramani SR, Gonzalez LC, Akashi-Takamura S, Miyake K, Zhang J, Lee WP, Muszyński A, *et al*: Noncanonical inflammasome activation by intracellular LPS independent of TLR4. Science 341: 1246-1249, 2013.
50. Knodler LA, Crowley SM, Sham HP, Yang H, Wrande M, Ma C, Ernst RK, Steele-Mortimer O, Celli J and Vallance BA: Noncanonical inflammasome activation of caspase-4/caspase-11 mediates epithelial defenses against enteric bacterial pathogens. Cell Host Microbe 16: 249-256, 2014.